Taylor & Francis
Taylor & Francis Group

Computer Methods in Biomechanics and Biomedical Engineering

ISSN: 1025-5842 (Print) 1476-8259 (Online) Journal homepage: https://www.tandfonline.com/loi/gcmb20

Estimation of mechanical power and energy cost in elite wheelchair racing by analytical procedures and numerical simulations

Pedro Forte, Daniel A. Marinho, Jorge E. Morais, Pedro G. Morouço & Tiago M. Barbosa

To cite this article: Pedro Forte, Daniel A. Marinho, Jorge E. Morais, Pedro G. Morouço & Tiago M. Barbosa (2018) Estimation of mechanical power and energy cost in elite wheelchair racing by analytical procedures and numerical simulations, Computer Methods in Biomechanics and Biomedical Engineering, 21:10, 585-592, DOI: 10.1080/10255842.2018.1502277

To link to this article: https://doi.org/10.1080/10255842.2018.1502277

COMPUTER METHODS IN BIOMECHANICS AND BIOMEDICAL ENGINEERING
2018, VOL. 21, NO. 10, 585–592
https://doi.org/10.1080/10255842.2018.1502277

Estimation of mechanical power and energy cost in elite wheelchair racing by analytical procedures and numerical simulations

Pedro Forte[a,b], Daniel A. Marinho[a,b], Jorge E. Morais[b,c], Pedro G. Morouço[d,e] and Tiago M. Barbosa[b,c,f]

[a]Department of Sport Sciences, University of Beira Interior, Covilhã, Portugal; [b]Research Centre in Sports, Health and Human Development, Covilhã, Portugal; [c]Department of Sport Sciences, Polytechnic Institute of Bragança, Bragança, Portugal; [d]Department of Sport Sciences, Polytechnic Institute of Leiria, Leiria, Portugal; [e]Centre for Rapid and Sustainable Product Development, Leiria, Portugal; [f]National Institute of Education, Nanyang Technological University, Singapore

ABSTRACT

The aim was to compare the mechanical power and energy cost of an elite wheelchair sprinter in the key-moments of the stroke cycle. The wheelchair-athlete system was 3D scanned and then computational fluid dynamics was used to estimate the drag force. Mechanical power and energy cost were derived from a set of formulae. The effective area in the catch, release and recovery phases were 0.41 m^2, 0.33 m^2 and 0.24 m^2, respectively. Drag increased with speed and varied across the key-moments. The catch required the highest total power (range: 62.76–423.46 W), followed-up by the release (61.50–407.85 W) and the recovery (60.09–363.89 W).

ARTICLE HISTORY
Received 21 September 2017
Accepted 16 July 2018

KEYWORDS
Drag; kinetics; paralympics; power output; sprinting

Introduction

In wheelchair racing, propulsive forces play an important role in the athlete's performance. Propulsive forces are produced by pushing the wheel's handrim periodically over a race (Forte et al. 2015). In a 100 m sprint, world-ranked wheelchair racers can perform about 40 full cycles of pushing the handrim (Barbosa and Coelho 2017). After each push, the athlete must reposition the hands on the handrim to perform another cycle (Forte et al. 2015; Barbosa and Coelho 2017). So, it is possible to breakdown each stroke cycle in two main phases: (i) propulsive phase and (ii) recovery phase. The propulsive phase is split-up in catch phase (the first contact of the hand on the handrim) and release phase (the moment the hand breaks off contact with the handrim). During the recovery phase, athletes usually perform an elbow flection and hyperextension of the shoulder to bring back the upper-arms forward and prepare a new push (Barbosa and Coelho 2017).

A sprinter aims to reach the resultant maximal velocity as soon as possible, and retain it throughout the race. The wheelchair-athlete system is considered more efficient if it can deliver less mechanical power and/or energy cost of transportation for a given velocity or pace (Forte et al. 2015; Barbosa et al. 2016; Hoffman et al. 2003). To reach the maximal velocity, energy is required to generate motion and overcome the resistive forces (Forte et al. 2015; Barbosa and Coelho 2017), thus:

$$v = \sqrt{\frac{2(E_{in} - E_{loss})}{m}} \quad (1)$$

where v is the wheelchair velocity, E_{in} the athlete delivered energy, E_{loss} the lost energy by the system and m the mass. The difference between E_{in} and E_{loss} encompasses the kinetic energy of the system (Barbosa et al. 2016).

In wheelchair racing, the main forces of energy lost (resistive forces) are the rolling friction and the drag force (Barbosa et al. 2016; Fuss 2009). Coaches and sports analysts aim to reduce the resistive forces as much as possible, to improve the final race time (Barbosa et al. 2016; Fuss 2009; Barbosa et al. 2014; Forte et al. 2016). Small shifts in the rider's position and the garments used can also help reducing the drag by about 10% (Barbosa et al. 2016; Forte et al. 2016; Rushby-Smith and Douglas 2012; Martin 1996; Forte et al. 2015). Nevertheless, the athlete's position varies over the stroke cycle. To produce propulsion, the athlete must bend the upper-body (i.e. torso and head) from a reasonably vertical to horizontal position, looking forward and arms pushing the handrim

CONTACT Pedro Forte pedromiguelforte@gmail.com Convento de Santo António, University of Beira Interior, 6201-001 Covilhã, Portugal

between the 12 and 18 h positions (these are known as the catch and release phases, respectively) (Forte et al. 2015). After the release, the athlete performs the recovery phase. The arms are back overstretched and will flex forward to prepare a new catch phase. Concurrently, the upper-body may do an extension reaching a slightly vertical position. The change in the upper-body and arms' position over the entire cycle is going to affect the drag force acting on the wheelchair-racer system (Forte et al. 2015; Forte et al. 2016).

At least in cycling, small variations in the bike-rider system have a meaningful effect on the aerodynamic drag (Martin 1996). However, there is scarce evidence on this matter in wheelchair racing (Barbosa et al. 2016; Candau et al. 1999). These drag changes in different positions of the stroke cycle may also affect the power and energy to reach maximal speed. At 1.80 m/s, the drag accounts to almost 5% of the total resistive forces, and ∼30% at 6.30 m/s (Barbosa et al. 2014). The rolling resistance accounts for 95% and 70% of the total resistive forces at 1.80 m/s and 6.30 m/s, respectively (Barbosa et al. 2014).

In wheelchair racing, it is possible to monitor the resistive forces by experimental testing (e.g. coast-down tests or wind tunnel), numerical simulations (e.g. computational fluid dynamics) and analytical models (a set of formulae) (MacLeish et al. 1993; Barbosa et al. 2014; Forte et al. 2015). Upon measuring the resistive forces and the inertial characteristics of the system, a set of analytical procedures can be used to estimate the mechanical work, power and energy (Wilson 2004). Assessing the changes in the resistive forces over the stroke cycle by any of the above mentioned methods (experimental testing, numerical simulations or analytical procedures), enables the estimation of the intra-cyclic variation of the mechanical work, power and energy in the key moments of the cycle (i.e. catch, release, recovery). As far as our understanding goes, this has not been yet reported in the literature. One previous study selected the same analytical procedure, but having inputs as data collected by coast-down technique (Barbosa et al. 2016). Nevertheless, Barbosa et al. (2016) aimed to compare the aerodynamics, mechanical work, power and energy at different racing positions (upright position, racing position with neck in flexion and racing position with neck in hyperextension) at a mean velocity of 6.298 m/s. As far as our understanding goes, this study is the first attempt to run such analysis based on computational fluid dynamics (CFD) and comparing the three key-moments of the stroke cycle.

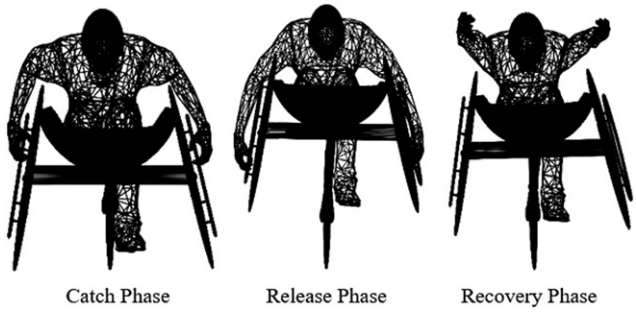

Figure 1. CAD model of the three different scanned positions: (i) catch phase; (ii) the release phase and; (iii) recovery phase respectively.

Hence, the aim was to compare the mechanical power and energy cost of transportation delivered by an elite wheelchair sprinter in the key-moments of the stroke cycle. It was hypothesized that: (i) the mechanical power and energy cost will vary at different key-moments of the stroke cycle, and; (ii) catch is the phase that demands more power and energy cost, followed-up by the release and then the recovery phases.

Methods

Participant

A male wheelchair sprinter competing in the T52 category was recruited for this research. He holds the national records in the 100 m and 400 m events, was a finalist at paralympic games and world championships in the same events and is an European medallist in the 100 m event. He was wearing his race suit and competition helmet. All procedures carried out in this research are in accordance with the Declaration of Helsinki. A written consent was obtained from the participant.

Scanning the model

The wheelchair-athlete system (49.16 kg) was 3D scanned (Artec Group, Inc., Luxembourg) in three different positions (Figure 1) of the stroke cycle (catch: with the hands on the handrims in the 12 h position; release: with the hands on the handrims in the 18 h position; recovery phase: with the arms hyperextended backwards and overstretched).

Artec studio 0.7 (Artec, U.S.A) software was used to record, smooth and merge all the scans. The geomagic studio (3D Systems, U.S.A) software was used to edit the merged scans into a single object without surface errors and then exported as a CAD model (*.iges) (Figure 1). Then, the model was imported in

Fluent code (Ansys Fluent 16.0, Ansys Inc., PA, U.S.A) to run the numerical simulations.

Boundary conditions

The entire domain featured 35 million prismatic and pyramidal elements. The grid node separation reduction in selected areas of high velocity and pressure, allowed to generate an accurate model (Bixler et al. 2007; Marinho et al. 2010). The domain was created in Ansys meshing module (Ansys Fluent 16.0, Ansys Inc., PA, U.S.A) with a tunnel form (3 m length, 2 m height and 1.5 m width). The Boolean subtract action was made to separate the wheelchair-athlete from the enclosure, this procedure defined that the wheelchair-athlete was an object (i.e. body) inside the tunnel. The described procedure was repeated for three key-moments of the stroke-cycle (i.e. catch, release and recovery phase).

The air velocity was set in the –z direction and in the inlet portion of the dome surface. The initial velocity of the numerical simulations was set at 2 m/s with increments of 1.5 m/s up to 6.5 m/s. The fluent (Ansys Fluent 16.0, Ansys Inc., PA, U.S.A), post process, allowed the estimation of the aerodynamic drag (Forte et al. 2015).

Numerical simulation

The CFD simulations encompassed the discretization of the Navier–Stokes equations by the finite volume approaches. The equations resulted from Newton's Second Law where, in mechanics, the fluid stress is the sum of the diffusion of its viscosity. This diffusion of its viscosity results from an applied pressure term (Marinho et al. 2012; Marinho et al. 2011). The Reynolds-averaged Navier–Stokes equation converts instantaneous values into means. The fluid flow behaviour (Equation 2), Reynolds stresses (Equation 3), temperature (Equation 4) and mass transfer (Equation 5) are then solved:

$$\frac{\partial_{\mathrm{Ui}}}{\partial_{\mathrm{xi}}} = 0 \tag{2}$$

$$\frac{\partial_{Ui}}{\partial_t} \pm U_j \frac{\partial_{Ui}}{\partial_{x_j}} = -\frac{1}{\rho}\frac{\partial P}{\partial x_j} + \frac{\partial}{\partial x_j}\left(2\nu S_{ij} - \overline{\mu_j'\mu_i'}\right) \tag{3}$$

$$\frac{\partial_{\theta i}}{\partial_t} \pm U_j \frac{\partial_{\theta}}{\partial_{x_j}} = \frac{1}{\rho_{cp}}\frac{\partial}{\partial x_j}\left(k\frac{\partial \theta}{\partial x_j} - \overline{\mu_j'\theta'}\right) \tag{4}$$

$$\frac{\partial_C}{\partial_t} \pm U_j \frac{\partial_C}{\partial_{x_j}} = \frac{\partial}{\partial x_j}\left(D\frac{\partial C}{\partial x_j} - \overline{\mu_j'c'}\right) \tag{5}$$

Fluent CFD code (Ansys Fluent 16.0, Ansys Inc., PA, U.S.A) was selected to run the above mentioned simulations. To represent the domain and fluid flow around the wheelchair-athlete system, a 3D grid or mesh with divided cells was formed in Ansys meshing module (Ansys Fluent 16.0, Ansys Inc., PA, U.S.A).

The realizable k-epsilon was selected as turbulence model. This model delivered velocity histograms identical to the standard k-e model, RST and RNG k-e model. Standard k-e, RST and RNG k-e models used to converge after 11,876, 3208 and 2874 interactions, respectively. Moreover, as far as computation economy is concerned, the realizable k-epsilon is much more efficient because the solutions converge after 1404 interactions (Pogni and Nicola 2016).

Drag force

Total aerodynamic drag (F_d) and frontal surface area were retrieved from Fluent code (Ansys Fluent 16.0, Ansys Inc., Pennsylvania, USA) software.

To compute the drag force, Equation (6) was used:

$$F_d = \frac{1}{2}\rho A C_D v^2 \tag{6}$$

where F_d is the drag force, C_D represents the drag coefficient, v the velocity, A the surface area and ρ is the air density. The effective area (AC_D) was calculated by the multiplying C_D by A. A was also extracted from Fluent software.

Mechanical power and energy cost

The power to overcome drag was calculated at the selected speeds as (Barbosa et al. 2016):

$$P_d = F_d.v_x \tag{7}$$

where P_d is the power to overcome drag, F_d the drag force and v_x the horizontal velocity.

A gross efficiency of 18% by wheelchair racers was assumed (Barbosa et al. 2016; Candau et al. 1999). The assumed rolling coefficient (CR) was 0.01 as reported for this same participant in an experimental testing (Barbosa et al. 2016; Barbosa and Coelho 2017). The power output (i.e. energy expenditure per unit of time), the energy cost (i.e. energy expenditure per unit of distance) and the external mechanical power delivered were estimated as (Cooper et al. 2003):

$$P_{tot} = \frac{CR.m.g.v + \frac{\rho}{2}.A.C_D.v^3}{n} \tag{8}$$

$$C = \frac{CR.m.g + \frac{\rho}{2}.A.C_D.v^2}{n} \tag{9}$$

$$P_{ext} = CR.m.g.v + \frac{\rho}{2}.A.C_D.v^3 \tag{10}$$

where P_{tot} is the total power, CR the rolling coefficient, m the body mass of the wheelchair-sprinter

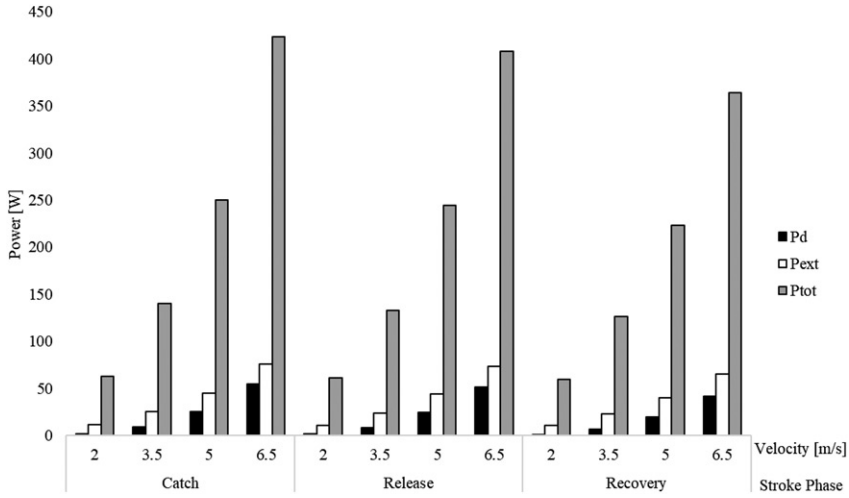

Figure 2. Power to overcome drag (P_d), external mechanical power (P_{ext}) and total power (P_{tot}) in the three key-moments of the stroke cycle at 2.0, 3.5, 5.0 and 6.5 m/s.

system, g the gravitational acceleration, v the mean velocity over the race, ρ the air density, A is the surface area and C_D the drag coefficient, C the energy cost, P_{ext} the external mechanical power and η the gross efficiency.

Results

Figure 2 reports the P_d, P_{tot}, C and P_{ext} per unit of distance in the key-moments of the stroke cycle at the selected speeds. The F_d increased with speed, ranging between 0.72 and 8.45 N. The recovery phase showed the lower drag intensity, followed by the release and then the catch phases. The F_d decreased from the catch to the release phase between 3% and 7% and, from the release to the recovery in ∼21–24%. The increase from the recovery to catch phase was 25–31%. The AC_D values were 0.24 m^2 in the recovery phase, 0.33 m^2 in the release phase and 0.41 m^2in the catch phase.

The power to overcome drag also increased with speed and ranged between 1.45 and 54.93 W. The recovery phase presented the lower power to overcome the drag, followed by the release phase. The catch phase presented the highest values. Between the catch and release phase, P_d decreased by ∼3– 7%. Between catch and recovery phase decreased by 25–31% and from the release to the recovery phases between 21% and 24%.

The total power varied from 60.09 to 423.46 W and increased with speed. The lowest values were observed in the recovery; whereas, the highest P_{tot} were noted in the catch phase. The differences between the catch and release were about 3% to 7% across selected speeds. The catch phase differed from the recovery phase by ∼8–21%. The differences between the release and recovery phases were about 4% to 15%.

The external mechanical power values ranged from 10.82to 76.22 W across the different positions and increased with speed. The phase showing less P_{ext} being delivered was the recovery. The catch phase presented the highest P_{ext}. The catch phase differed from the release phase by ∼3–8% and from the recovery phase ∼7–21%. Between the release and recovery phase, differences were ∼4–15%.

The C ranged between 33.33 and 276.26 J/m (Figure 3). The key-moment that demanded less C, at the selected speeds, was the recovery phase; conversely, the catch phase demanded the highest cost. From the catch to the release, differences were ∼6–12%. From the catch to the recovery phase, C decreased between 13% and 30%. The release phase differed from recovery phase by ∼6–21%.

Discussion

The aim of this study was to compare the mechanical power and energy cost of transportation delivered by an elite wheelchair sprinter in key-moments of the stroke cycle. The main findings were that: (i) the mechanical power and energy cost of transportation varied in the different key-moments of the stroke cycle; (ii) the catch was the phase that required more power and energy cost followed-up by the release and then the recovery phases.

A wheelchair for team sports was noted as having a CR between 0.015 on a carpet, and 0.005 on wood floor (Chua et al. 2010). A standard wheelchair had a different CR on hard surface, smooth surface and carpet, depending of the wheel's type (0.001 in soft caster

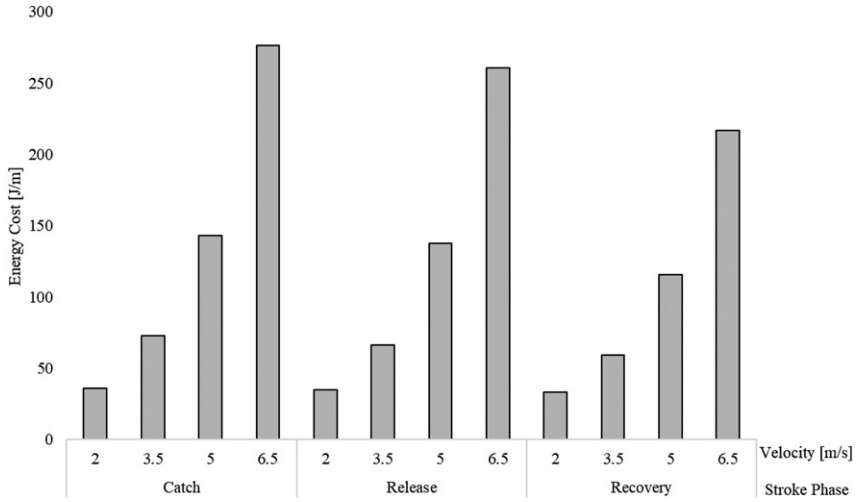

Figure 3. Energy cost in the three key-moments of the stroke cycle at 2.0, 3.5, 5.0 and 6.5 m/s.

on hard and smooth surfaces and 0.007 of solid tire on a carpet) (Sauret et al. 2012). Similar *CR* was reported for five different types of wheelchairs on linoleum and carpet (0.0013 on linoleum for a racing wheelchair and 0.0212 of a folding wheelchair on linoleum) (McLean et al. 1994). Our assumption was a CR of 0.01 as measured by experimental testing on this same participant early on (Barbosa and Coelho 2017; Barbosa et al. 2016; Hoffman et al. 2003). Other assumptions were a temperature of 15 °C and density of 1.225 kg/m^3. This same temperature and density were also noted by Blocken et al. (2016) for road cycling. Indeed, this environmental conditions are Fluent's default values (Ansys Fluent 16.0, Ansys Inc., PA, U.S.A) (ANSYS, 2013). Gross efficiency was assumed to be 18% as noted in the literature (Cooper et al. 2003; Vanlandewijck and Thompson 2011). For example, Cooper et al. (2003) tested 12 elite wheelchair racers on a computer monitored wheelchair dynamometer. The authors reported a gross mechanical efficiency of 18% as well. Vanlandewijck and Thompson (2011), also reported a gross mechanical efficiency of wheelchair racers between 15% and 23%.

The drag ranged between 0.72 and 8.45 N. These results seem to match the range reported using cost-down techniques (Barbosa et al. 2016; Hoffman et al. 2003). Hoffman et al. (2003) noted an AC_D of 0.37 m^2. Barbosa et al. (2016) studied the AC_D of a racing wheelchair in three different racing positions by cost-down and photogrammetric techniques. The AC_D ranged between 0.1456 and 0.1747 m^2. In cycling and wheelchair racing it is noted that small variations in the rider's positions may influence drag by about 10% (Rushby-Smith and Douglas 2012 and; Martin 1996; McLean et al. 1994). The AC_D ranged between 0.24 and 0.41 m^2. These values seem to be in accord with findings by Hoffman et al. (2003). Even so, in our research, at 6.5 m/s, the differences between the AC_D and the values reported by Barbosa et al. (2016), at a racing position was almost 0.2 m^2. The difference can be explained by the testing techniques selected (numerical simulations vs cost-down), testing conditions (comparison of the key-moments in the stroke cycle vs comparison of different racing positions) and inputs or assumptions (e.g. different climacteric conditions selected as inputs). The AC_D values in our study are dependent of athlete's anthropometry and individual characteristics. The catch phase showed the highest F_d. It differed from the release between 3% and 7% and from the recovery between 25% and 31%. The release phase had higher values than recovery in about 21% to 24%. These differences can be explained by the surface area in the different phases of the stroke cycle. The catch phase had a larger surface area when compared to the release; whereas, the release phase had a larger surface in comparison to the recovery phase. The increase in surface area in the catch phase might be due the arms position (elbow flection and with lateral projection). In the release phase, the subject upper-limbs were stretched and closed to the handrims. In the recovery phase, the upper limbs were over-stretched backwards.

The power to overcome the resistive forces had been studied in wheeled vehicles (Barbosa et al. 2016; Hoffman et al. 2003; Candau et al. 1999). In cycling, the P_d ranged between 10 W at 1.2 m/s and 80 W at 5.5 m/s (Candau et al. 1999). In wheelchair racing, Barbosa et al. (2016) reported that less power was needed to overcome the drag in the racing positions with the neck in hyperextension (22.19 W). In this study, in a similar position and at 6.5 m/s the power to overcome the drag was 54.93 W. Firstly, the relationship between power and speed is cubed ($P_d = D,v = k.v^2$, $v = k.v^3$). Secondly,

the AC_D reported by these authors was smaller than the one obtained in this study. The chair and garment used by the athlete was different in both studies. Others aimed to assess the resistive forces by coast-down in different types of wheelchairs (Hoffman et al. 2003). In a racing wheelchair at 5 m/s, P_d was 35 W. However, after the acceleration the subject placed the hands on his knees and the torso was kept in the upright position (Hoffman et al. 2003). This position increases the surface area and hence, the P_d. Despite the difference, and considering that the subject was not in a racing position, the results seem to match ours. At 5 m/s, the P_d was 25.59 W, 24.45 W and 19.67 W in the catch, release and recovery phases, respectively. Between positions, the catch phase had the highest P_d, followed by the release and then the recovery phase. P_d is dependent on the speed and F_d (Equation 6). Thus, a poor aerodynamic position will require an increase in the P_d.

Barbosa et al. (2016) reported a total power between 602.55 W and 630.71 W at 6.238 m/s in different racing positions. Pelland-Leblanc et al. (2013) noted the power transfer evaluated by an optical encoder on a track, reporting a mean value of 555 W at 5.34 m/s. These results seem to match what was obtained at 6.5 m/s. Breaking down by key-moments of the stroke phase, the catch phase demanded the highest P_{tot} and the recovery the lowest. The catch phase presented a higher drag due the arms position near the handrims. The elbows flexion and abduction in the catch phase increased the wheelchair-athlete's width. A higher width may lead to a higher surface area and a higher P_{tot} is required to surpass drag. In our study, P_{tot} increased with speed.

The energy cost reported by Barbosa et al. (2016) ranged between 95.67 and 100.14 J/m. Abel at al. (2003) assessed the energy cost on handbiking and wheelchair racing by spirometry in an endurance test. At almost 6 m/s, the C was on average 95.55 ± 19.14 J/m. These results seem to be in tandem to our data (Figure 3). Therefore, our estimation seems to be a good approximation. At 5 m/s the C ranged between 142.98 and 115.99 J/m, depending on the position adopted. The catch phase imposed the highest energy cost in comparison to release and recovery phases. The recovery phase led to the lowest energy cost. As there is no propulsion being applied on the handrim, one may argue that the C should be almost null, or at least, neglectable. Nevertheless, the wheelchair-athletes system keeps its motion due to inertia. Thus, the system's motion will not stop unless the resistive forces overcome the inertial force. At each propulsive phase, the inertial force increases, keeping the wheels in motion during the recovery phase. In our study, the C increased with speed. Also in handbiking, the C increased with speed (Abel et al. 2003). In cycling, it was possible to observe that different positions lead to a higher or lower energy cost (Ryschon and Stray-Gundersen 1991). The standing position presented a higher energy cost compared to a sitting position when monitored by the measurement of the oxygen uptake. The standing position presented a larger surface area and a higher energy cost. In our study the position with the largest effective area also denoted the highest energy cost.

The external mechanical power ranged between 10.82 and 76.22 W. Barbosa et al. (2016), noted a variation between 108.51 and 113.59 W for different racing positions. It is important to point out that the authors presented a higher P_{ext} in comparison to our results. In a study on basketball wheelchairs, the P_{ext} was evaluated on a roller ergometer in two different time periods (Theisen et al. 1996). The mean P_{ext} was calculated for 15 cycles in each stage and was computed by the momentary torque and angular velocity in the rear wheels. The exercise test was continuous with stages of 3 min. The subjects started at the tests at 0.58 m/s with increments of 0.28 m/s. The subjects did not reach their maximal capacity in the same stage, four reached 1.94 m/s, six reached 2.22 m/s and one was able to continue up to 2.50 m/s. P_{ext} values ranged between 12 and 63 W over the incremental protocol. The mean P_{ext} values were 50.92 ± 6.02 W and 50.73 ± 5.74 W. In our study, P_{ext} ranged between 10.82 and 11.30 W at 2 m/s, which might be explained by the fact that racing wheelchairs require less power to reach a higher speed. The maximal speed reached in basketball wheelchair was 2.5 m/s and in racing wheelchair almost 7 m/s.

Altogether, the AC_D and speed play important roles in F_d, P_d, P_{tot}, C and P_{ext} (Equations 6–10)). The evaluated variables increased with speed. This was expected since F_d, P_d, P_{tot}, C and P_{ext} are speed dependents. The variables also varied at different key-moments of the stroke cycle that was explained by the effective area differences between positions. Positions with higher surface area and effective area lead to higher drag and required a higher P_d, P_{tot}, C and P_{ext} to surpass the resistive forces.

Athletes' technique and muscle strength are determinants to deliver maximal power. So, they must be advised to enhance muscular strength and power, to perform explosive pushes in each stroke cycle (Barbosa and Coelho 2017). In the 100 m event in the T52 category, it is hard to reach the maximal

muscular power and speed due to the athletes' handicap. Thus, they must start the race performing, faster and explosive pushes (Barbosa and Coelho, 2017). For instance, these results may help coaches and athletes to design training sets at the required muscle power for a given speed or pace (i.e. sets of 15 s at 423 W).

The main limitations of this study were: (i) a set of assumptions were used to run the calculations (the rolling resistance, temperature, density and gross efficiency); (ii) the participant recruited is only representative of world-class athletes and not counterparts of other tiers; (iii) a comparison of mechanical power and energy cost estimation by numerical simulations and experimental testing (e.g. wind tunnel) is suggested.

Conclusion

The resistance acting upon the wheelchair racing sprinter increased with speed and varied across the different key-moments of the stroke cycle. The mechanical power and energy cost increased with speed. The phase demanding more power and energy cost was the catch phase, followed-up by the release and then the recovery phases. Athletes should maintain a proper body alignment and synchronization during the stroke cycles, enabling to reach and keep a maximal speed with a lower energy cost. Coaches and other practitioners can use these findings to carry out and evidence-based practice helping the athletes to improve their efficiency.

Disclosure statement

No potential conflict of interest was reported by the authors.

Funding

This project was supported by the National Funds [FCT - Portuguese Foundation for Science and Technology (UID/DTP/04045/2013)] and the European Fund for regional development (FEDER) allocated by European Union through the COMPETE 2020 Programme

ORCID

Pedro Forte http://orcid.org/0000-0003-0184-6780

References

Abel T, Kröner M, Rojas VS, Peters C, Klose C, Platen P. 2003. Energy expenditure in wheelchair racing and handbiking-a basis for prevention of cardiovascular diseases in those with disabilities. Euro J of Cardio Prev Rehab. 10(5):371–376.

ANSYS Inc. 2013. ANSYS fluent tutorial guide.Southpointe, PA: ANSYS Inc.

Barbosa TM, Coelho E. 2017. Monitoring the biomechanics of a wheelchair sprinter racing the 100 m final at the 2016 paralympic games. Euro J of Phy. 38(4):044001.

Barbosa TM, Forte P, Estrela JE, Coelho E. 2016. Analysis of the aerodynamics by experimental testing of an elite wheelchair sprinter. Procedia Eng. 147:2–6.

Barbosa TM, Forte P, Morais JE, Coelho E. 2014. Partial contribution of rolling friction and drag force to total resistance of an elite wheelchair athlete. Proceedings of the 1st International Conference in Sports Science & Technology; Dec 11–12; Singapore: Institute of Sports Research. p. 749–753

Bixler B, Pease D, Fairhurst F. 2007. The accuracy of computational fluid dynamics analysis of the passive drag of a male swimmer. Sports Biomechanics. 30(2):81–98.

Blocken B, Toparlar Y,and Andrianne T. 2016. Aerodynamic benefit for a cyclist by a following motorcycle. J of Wind Eng and Ind Aero. 155:1–10.

Candau RB, Grappe FR, Ménard MA, Barbier BR, Millet GY, Hoffman MD, Belli AR, Rouillon JD. 1999. Simplified deceleration method for assessment of resistive forces in cycling. Med Sci Sports Exerc. 31:1441–1447.

Chua JJ, Fuss FK, Subic A. 2010. Rolling friction of a rugby wheelchair. Procedia Eng. 2(2):3071–3076.

Cooper RA, Boninger ML, Cooper R, Robertson RN, Baldini FD. 2003. Wheelchair racing efficiency. Disability and rehab. 1(25):207–212.

Forte P, Barbosa TM, Marinho DA. 2015. Technologic appliance and performance concerns in wheelchair racing – helping paralympic athletes to excel. In: Chaoqun L, editor. New perspectives in fluid dynamics. Vila Real, Portugal: IEEE.

Forte P, Marinho DA, Morouço PG, Barbosa T. 2016. CFD analysis of head and helmet aerodynamic drag to wheelchair racing. Paper presented at: 1st International Conference on Technology and Innovation in Sports, Health and Wellbeing (TISHW); International Conference. Vila Real, Portugal: IEEE.

Fuss FK. 2009. Influence of mass on the speed of wheelchair racing. Sports Eng. 12:41–53.

Hoffman MD, Millet GY, Hoch AZ, Candau RB. 2003. Assessment of wheelchair drag resistance using a coasting deceleration technique. Am J Physical Med & Rehab. 82(11):880–889.

MacLeish MS, Cooper RA, Harralson J, Ster JF. 1993. Design of a composite monocoque frame racing wheelchair. J of rehab res and dev. 30:233.

Marinho DA, Barbosa TM, Mantha V, Rouboa AI, Silva AJ. 2012. Modelling propelling force in swimming using numerical simulations. In: Juarez LH, editor. Fluid dynamics, computational modeling and applications. p. 439–448. London: InTech.

Marinho DA, Barbosa TM, Reis VM, Kjendlie PL, Alves FB, Vilas-Boas JP, Machado L, Silva AJ, Rouba AI. 2010. Swimming propulsion forces are enhanced by a small finger spread. J of Appl Biomech. 26(1):87–92.

Marinho DA, Silva AJ, Reis VM, Barbosa TM, Vilas-Boas JP, Alves FB, Machado L, Rouboa A. 2011. Three-dimensional

CFD analysis of the hand and forearm in swimming. J of App Biomech. 27(1):74–80.
Martin JC. 1996. Aerodynamics and cycling. Mast Athl Physio and Perform 1:1–6.
McLean BD, Danaher R, Thompson L, Forges A, Coco G. 1994. Aerodynamic characteristics of cycle wheels and racing cyclists. J of Biomech. 27:675.
Pelland-Leblanc JP, Martel F, Langelier È, Smeesters C, Berrigan F, Laroche J, Rancourt D. 2013. Instantaneous power measurement in wheelchair racing. Paper presented at: 37th Annual Meeting of the American Society of Biomechanics; Omaha, Nebraska, USA.
Pogni M, Nicola P. 2016. Comparison of the aerodynamic performance of five racing bicycle wheels by means of CFD calculations. Procedia Eng. 147:74–80.
Rushby-Smith T, Douglas L. 2012. Paralympic technology. Ingenia. 51:33.
Ryschon TW, Stray-Gundersen J. 1991. The effect of body position on the energy cost of cycling. Medicine and science in sports and exercise. 23(8):949–953.
Sauret C, Bascou J, de Saint Rémy N, Pillet H, Vaslin P, Lavaste F. 2012. Assessment of field rolling resistance of manual wheelchairs. J Rehab Res Development. 49(1):63–74.
Theisen D, Francaux M, Fay A, Sturbois X. 1996. A new procedure to determine external power output during handrim wheelchair propulsion on a roller ergometer: a reliability study. Int J of Sports Med. 17(8):564–571.
Vanlandewijck YC, Thompson WR. 2011. Handbook of sports medicine and science, the paralympic athlete. Oxford, United Kingdom:Wiley-Blackwell.
Wilson DG. 2004. Bicycling science. Cambridge, MA: MIT Press Bicycle aerodynamics; p. 188.